

Szymon Tengler (stengler@ath.bielsko.pl)

Department of Mechanics, University of Bielsko-Biala

Kornel Warwas

Department of Computer Science and Engineering, University of Bielsko-Biala

DRIVER COMFORT IMPROVEMENT BY A SELECTION OF OPTIMAL SPRINGING OF A SEAT

POPRAWA KOMFORTU KIEROWCY POPRZEZ DOBÓR OPTIMALNEGO RESOROWANIA FOTEŁA

Abstract

An optimal way to select parameters of a driver's seat of a special vehicle, which contributes directly to an increase in driving comfort is presented in the work. A mathematical model of the vehicle was formulated by using of joint coordinates and homogenous transformations. A maneuver of driving over obstacles in a form of a speed bump of different heights and lengths is presented. A subject of the investigations was to select such damping parameters and driver's seat stiffness to minimize amplitudes of vibrations present in this sub-assembly. An influence of a form of an objective function and a selection of decisive variables on quality of the optimization results obtained was analyzed.

Keywords: active suspension, drive comfort, dynamic optimization, computer modeling

Streszczenie

W pracy przedstawiono sposób doboru optymalnych parametrów fotela kierowcy pojazdu specjalnego, który bezpośrednio przyczynia się do zwiększenia komfortu jazdy. Model matematyczny pojazdu sformułowano korzystając ze współrzędnych złączowych i przekształceń jednorodnych. Przedstawiono manewr przejazdu przez przeszkody w postaci progów zwalniających o różnej wysokości i długości. Przedmiotem badań było dobranie takich parametrów tłumienia i sztywności fotela kierowcy, aby zminimalizować amplitudy drgań występujące w tym podzespołe. W pracy skoncentrowano się na analizie wpływu postaci funkcji celu oraz doboru zmiennych decyzyjnych na jakość uzyskanych wyników optymalizacyjnych.

Słowa kluczowe: aktywne zawieszenie, komfort jazdy, optymalizacja dynamiczna, modelowanie komputerowe

1. 1. Introduction

Driving comfort of a driver and passengers in the motor vehicles is a subject of considerations of many scientific and research papers [1, 2, 3, 4]. A comfort improvement can have a significant influence on both effective time of vehicle use and a level of operator tiredness. It is particularly important in the case of articulated and special vehicles in which an operator spends daily on average from a few to over a dozen hours [2]. A lot of research deals with human-seat interaction [5, 6, 7]. In these works authors focus on accurate modelling of human body with seat contact. The presented research deals with truck drivers considering travel time factor and designing best possible alternatives of driver's seat shape. In order to this objective they used the aid of ergonomics and advanced design tools like CAD CAE and FEM (ABAQUS). As it is shown in [8, 9, 10] the comfort improvement of a driver and passengers is frequently identified with modifications of vehicle sub-assemblies. In this case researchers do not include the human body interaction but they are focused on changes and improvements in the vehicle elements such as suspension, and those systems are commonly called an active or semi-active suspension [1, 9, 10]. In the paper [11] the optimization of damping in the passive suspension system of a vehicle moving on a road with rough surface of random irregularities, described according to the ISO classification has been presented. The optimum suspension damping coefficient was determined. Seats, and in particular a driver's seat, are a next sub-assembly which has a direct influence on the driving comfort [12]. In this case a reduction of the vibrations occurring while driving over the uneven road surfaces can turn out to be an important factor affecting the driving comfort improvement [13]. An influence of uneven road surfaces on the driver seat behavior is presented as an example in paper [14]. The authors used a magneto-rheological shock absorber to improve driving comfort. Regulators and actuators which must be calibrated properly, are usually used to select optimum parameters of the sub-assemblies [1, 9, 10]. The selection of the appropriate parameters of the vehicle sub-assemblies can be also made by solving an optimization task. So far these methods have been used, among other things, in papers [15, 16] to solve tasks in a scope of controlling the systems supporting a driver in dangerous road situations. The authors used methods of a different degree of numerical complexity to select braking torques acting on a particular wheel of the vehicle. Optimization performed in this scope aimed at calibrating and testing the existing systems. During the optimization a functional defined in a form of the integral criterion was minimized. In order to solve an issue how to select proper values of the driver's seat sub-assembly parameters, different methods of dynamic optimization were used in paper [17] and analyses were made related to a selection of the functional used in the optimization task. An objective function and its influence on the final values of the dynamic optimization task obtained and time of the simulation calculations were analyzed.

In this article different objective function forms and decisive variable variants were subjected to an analysis and their influence on the results obtained in the optimization process was investigated. The investigations concerned an improvement of comfort of driving by a special vehicle for the assumed road maneuver with obstacles in a form of speed bumps. A special models of road surface and own authors algorithms to determine position of contact point of tire with road surface where acting reaction forces have been used [18, 19]. To obtain these reactions tire model Fiala was used [20].

It is worth to emphasising that in [21, 22, 23] the similar analysis using evaluation algorithms have been performed. However, the road unevenness was modelled as sinusoidal function and mathematical models of vehicles have reduced the numerical complexity.

2. Mathematical model

An object of testing is a rescue fire-fighting vehicle being an example of a vehicle with a high gravity center. In the analyzed vehicle there were twelve sub-assemblies identified such as: a frame, a cabin, a driver's seat, a body, an engine, a front and rear axle, stub axles and wheels (Fig. 1).

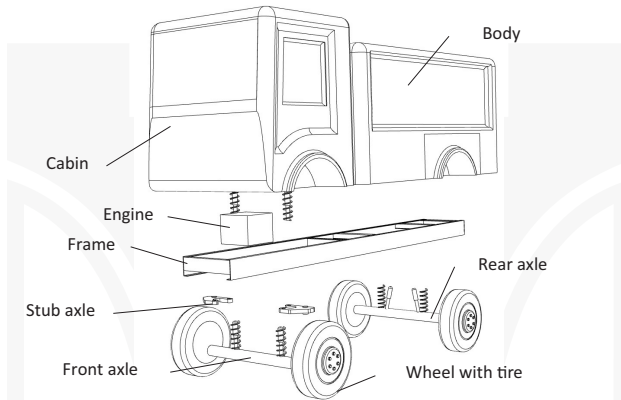


Fig. 1. Parts of the vehicle

Joint coordinates and homogenous transformations were used to determine a position and orientation of these bodies in the three-dimensional space [15, 17, 24]. At such a way of modeling motion of each body (except for the base body), is determined in relation to a preceding body, and this motion is described by the generalized coordinates assumed appropriately. For the frame model (Fig. 2), the vector of the generalized coordinates has the following form:

$$\tilde{\mathbf{q}}^{(1)} = [\tilde{x}^{(1)} \tilde{y}^{(1)} \tilde{z}^{(1)} \tilde{\psi}^{(1)} \tilde{\theta}^{(1)} \tilde{\varphi}^{(1)}]^T \quad (1)$$

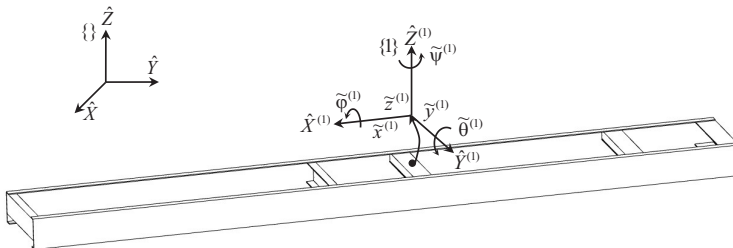


Fig. 2. A model of the vehicle frame

The cabin (Fig. 3) is mounted to the frame and in relation to it the cabin has one degree of freedom (a rotation):

$$\tilde{\mathbf{q}}^{(2)} = [\theta^{(2)}] \quad (2)$$

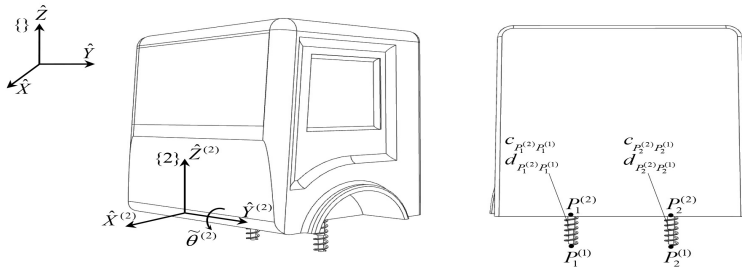


Fig. 3. The cabin model

The model of driver's seat is presented in Fig. 4.

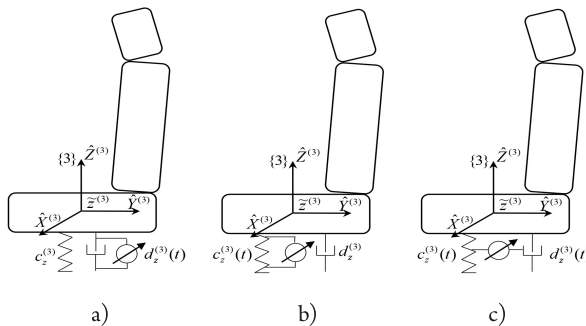


Fig. 4. The driver's seat model for controlling: a) damping, b) stiffness, c) damping and stiffness

It has one degree of freedom and is connected with the cabin by a spring and a damper:

$$\tilde{\mathbf{q}}^{(3)} = [\tilde{z}^{(3)}] \quad (3)$$

The seat surface amortization and contact between a driver and a seat have been simplified. The influence of these phenomenon has been taken into account in $c_z^{(3)}$ and $d_z^{(3)}$ coefficients. Models of the front and rear axles are presented in Fig. 5. Each of the axles in relation to the frame has three degrees of freedom – two displacements and one rotation. The displacements are determined by generalized coordinates $\tilde{y}^{(4)}, \tilde{z}^{(4)}$ (in the case of the front axle) $\tilde{y}^{(5)}, \tilde{z}^{(5)}$ (in the case of the rear axle), whereas the rotations – coordinate $\tilde{\theta}^{(4)}$ (in the case of the front axle), $\tilde{\theta}^{(5)}$ (in the case of the rear axle), respectively. A role of suspension springs is played by elastic elements mounted between the determined points. Operating of torque control rods is modeled by the elastic elements of deformation directions compatible with generalized

coordinates $\tilde{\theta}^{(4)}$ and $\tilde{\theta}^{(5)}$. The suspension springs of the vehicle are characterized by lateral flexibility, therefore translating elastic elements acting in the direction consistent with generalized coordinates $\tilde{y}^{(4)}$ and $\tilde{y}^{(5)}$ were implemented into the mathematical model.

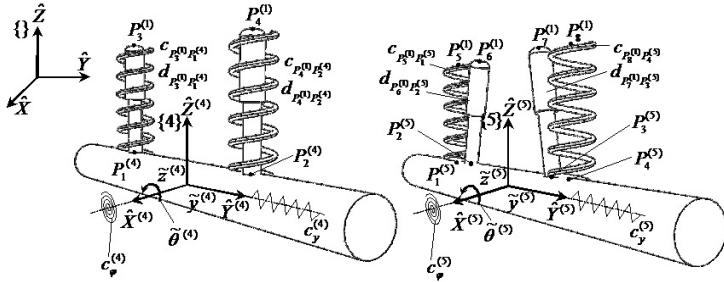


Fig. 5. Models of the axles

Vectors of the generalized coordinates of the axles are as follows:

$$\tilde{\mathbf{q}}^{(4)} = [\tilde{y}^{(4)} \tilde{z}^{(4)} \tilde{\theta}^{(4)}]^T \quad (4)$$

$$\tilde{\mathbf{q}}^{(5)} = [\tilde{y}^{(5)} \tilde{z}^{(5)} \tilde{\theta}^{(5)}]^T \quad (5)$$

The stub axles in relation to the front axle can make a rotation (Fig. 6), and their vectors of the generalized coordinate take a form of:

$$\tilde{\mathbf{q}}^{(6)} = [\tilde{\psi}^{(6)}] \quad (6)$$

$$\tilde{\mathbf{q}}^{(7)} = [\tilde{\psi}^{(7)}] \quad (7)$$

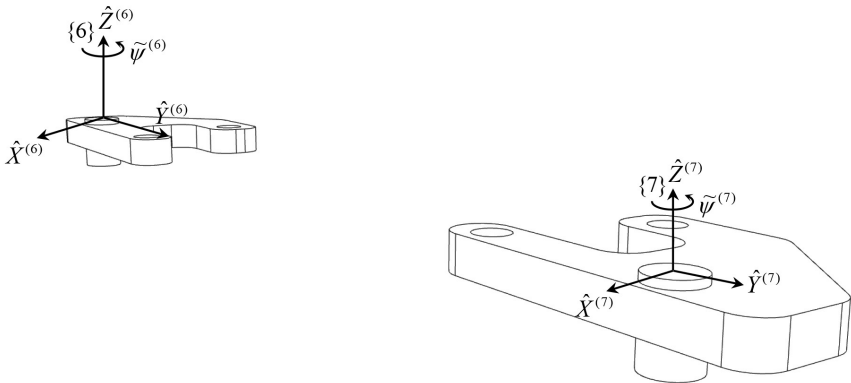


Fig. 6. Models of the stub axles

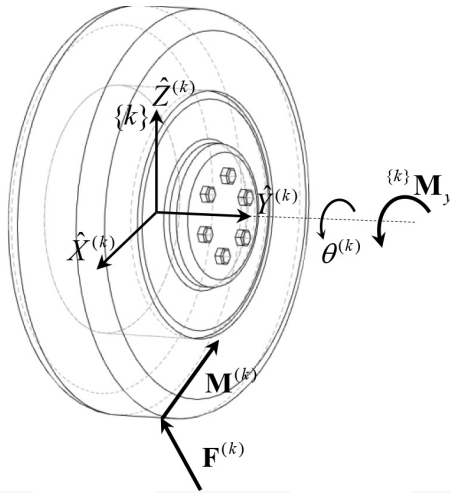


Fig. 7. A model of the wheel

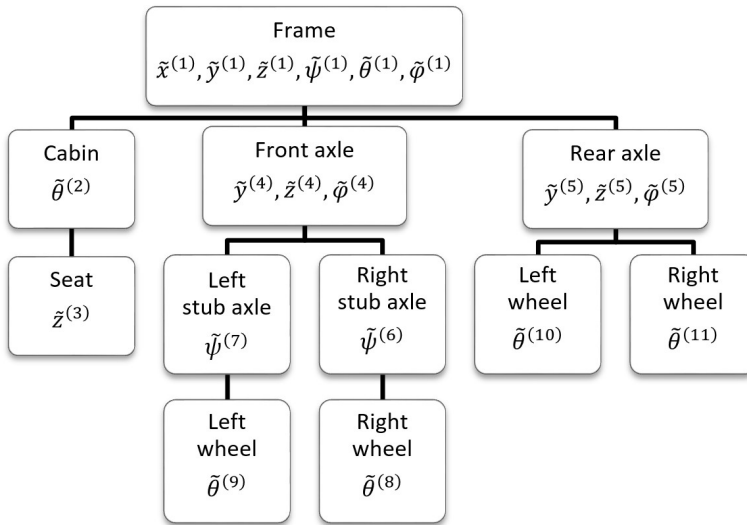


Fig. 8. Models of the sub-assemblies forming the tree structure of the considered multibody system

The front wheels (mounted to the stub axles) and the rear wheels (mounted to the axle) have one degree of freedom in relation to the preceding bodies – a rotation. Models of the wheels (bodies no 8, 9, 10, 11) are presented in Fig. 7.

Their vectors of the generalized coordinates are as follows:

$$\tilde{\mathbf{q}}^{(k)} = [\tilde{\theta}^{(k)}] \quad (8)$$

Force $F^{(k)}$ and moment $M^{(k)}$ of a couple of forces, constituting a reaction of a road surface, and driving torque moment ${}^{(k)}M_y$, located in the axis of rotation of the rear wheels act on the particular wheel k . Components of forces $F^{(k)}$ and moment $M^{(k)}$, were determined by the Fiala tire model [18, 20]. These components are applied to the contact point, specified in paper [18], of the tire model with the road surface. The road is discretized, and both the detailed algorithms for modeling surface unevenness and the algorithms which enable to determine a position of contact point C in the reference system $\{ \}$ are presented in [18]. Driving torque moments ${}^{(k)}M_y$ act on the rear wheel of the vehicle ($k=10,11$) according to a principle of the open symmetrical differential mechanism. Appropriate driving torques controlled by a PID regulator are provided to the vehicle wheels in order to ensure the desired speed of the vehicle. The last sub-assemblies of the vehicle are the engine and the body. They are modeled as bodies connected rigidly with the frame, therefore they do not have relative generalized coordinates. The multibody system can be presented as a tree structure which contains the open kinematic chains (Fig. 8). Nodes of this tree are bodies modeling a specifying sub-assemblies.

Equations of vehicle motion have been formulated using Lagrange equations of the second kind [15, 18]:

$$\frac{d}{dt} \frac{\partial E}{\partial \dot{q}_k} - \frac{\partial E}{\partial q_k} + \frac{\partial V}{\partial q_k} + \frac{\partial V_D}{\partial \dot{q}_k} = Q_k \quad (9)$$

where:

$E = \sum_{p=1}^N E^{(p)}$ – total kinetic energy of the vehicle,

$E^{(p)}$ – kinetic energy of the p -th body,

$V = \sum_{p=1}^N V^{(p)}$ – total potential energy of the vehicle,

$V^{(p)}$ – potential energy of the p -th body,

$V_D = \sum_{p=1}^N V_D^{(p)}$ – total energy dissipation function of the vehicle,

$V_D^{(p)}$ – energy dissipation function of the p -th body,

$\dot{q} = \frac{dq}{dt} = (\dot{q}_k)_{k=1, \dots, n}$ – vector of generalized velocities of the system,

$Q = (Q_k)_{k=1, \dots, n}$ – vector of generalized forces of the system,

N – number of bodies of the vehicle,

n – number of generalized coordinates of the vehicle,

$k = 1, \dots, n$.

Using transformations described in [15, 18, 24] the components of kinetic energy of p -th body can be formulated as:

$$\frac{d}{dt} \frac{\partial E^{(p)}}{\partial \dot{\mathbf{q}}_i^{(p)}} - \frac{\partial E^{(p)}}{\partial \mathbf{q}_i^{(p)}} = \text{tr} \left\{ \mathbf{B}_i^{(p)} \mathbf{H}^{(p)} \ddot{\mathbf{B}}^{(p)\top} \right\} \quad (10)$$

where:

$\mathbf{B}^{(p)}$ – transformation matrix of the p -th body in relation to inertial system,

$$\mathbf{B}_i^{(p)} = \frac{\partial \mathbf{B}^{(p)}}{\partial \mathbf{q}_i^{(p)}},$$

$$\mathbf{H}^{(p)} = \left(h_{i,j}^{(p)} \right)_{i,j=1,\dots,4} = \begin{bmatrix} \int_m \tilde{x}^2 dm & \int_m \tilde{x}\tilde{y} dm & \int_m \tilde{x}\tilde{z} dm & \int_m \tilde{x} dm \\ \int_m \tilde{y}\tilde{x} dm & \int_m \tilde{y}^2 dm & \int_m \tilde{y}\tilde{z} dm & \int_m \tilde{y} dm \\ \int_m \tilde{z}\tilde{x} dm & \int_m \tilde{z}\tilde{y} dm & \int_m \tilde{z}^2 dm & \int_m \tilde{z} dm \\ \int_m \tilde{x} dm & \int_m \tilde{y} dm & \int_m \tilde{z} dm & \int_m dm \end{bmatrix}$$

– pseudo inertia matrix defined in the local coordinate system of p -th body,

m – mass of the p -th body,

$\tilde{x}, \tilde{y}, \tilde{z}$ – coordinates of location described in local coordinate system of the p -th body,

$\text{tr}\{\mathbf{M}\}$ – trace of the matrix \mathbf{M} .

After transformations dynamic equations of motion of the p -th sub-system of the vehicle can be written in the general form:

$$\mathbf{A}^{(i)}(t, \mathbf{q}) \ddot{\mathbf{q}}^{(i)} = \mathbf{f}^{(i)}(t, \mathbf{q}, \dot{\mathbf{q}}) \quad (11)$$

where:

$\mathbf{A}^{(i)}$ – mass matrix,

$\mathbf{f}^{(i)}$ – vector of external, Coriolis, centrifugal and gravity forces.

Therefore equations of motion of the particular sub-system of the vehicle can be described as follow:

- ▶ sub-system 1 (frame – F, front axle – AF, stub axle – SA, front wheels – WF)

$$\mathbf{A}^{(1)} = \begin{bmatrix} \mathbf{A}_{F,F}^{(1)} & \mathbf{A}_{F,AF}^{(1)} & \mathbf{A}_{F,SA}^{(1)} & \mathbf{A}_{F,Wf}^{[1]} \\ \mathbf{A}_{AF,F}^{(1)} & \mathbf{A}_{AF,AF}^{(1)} & \mathbf{A}_{AF,SA}^{(1)} & \mathbf{A}_{AF,Wf}^{(1)} \\ \mathbf{A}_{SA,F}^{(1)} & \mathbf{A}_{SA,AF}^{(1)} & \mathbf{A}_{SA,SA}^{(1)} & \mathbf{A}_{SA,Wf}^{(1)} \\ \mathbf{A}_{Wf,F}^{(1)} & \mathbf{A}_{Wf,AF}^{(1)} & \mathbf{A}_{Wf,SA}^{(1)} & \mathbf{A}_{Wf,Wf}^{(1)} \end{bmatrix}, \quad \mathbf{q}^{(1)} = \begin{bmatrix} \tilde{\mathbf{q}}^{(1)} \\ \tilde{\mathbf{q}}^{(4)} \\ \tilde{\mathbf{q}}_{SA}^{(1)} \\ \tilde{\mathbf{q}}_{Wf}^{(1)} \end{bmatrix}, \quad \mathbf{f}^{(1)} = \begin{bmatrix} \mathbf{f}_F^{(1)} \\ \mathbf{f}_{AF}^{(1)} \\ \mathbf{f}_{SA}^{(1)} \\ \mathbf{f}_{Wf}^{(1)} \end{bmatrix}$$

$$\text{where: } \tilde{\mathbf{q}}_{SA}^{(1)} = \begin{bmatrix} \tilde{\Psi}^{(6)} \\ \tilde{\Psi}^{(7)} \end{bmatrix}, \quad \tilde{\mathbf{q}}_{Wf}^{(1)} = \begin{bmatrix} \tilde{\Theta}^{(1)} \\ \tilde{\Theta}^{(2)} \end{bmatrix}$$

- ▶ sub-system 2 (frame – F, rear axle – AR, rear wheel – WR)

$$\mathbf{A}^{(2)} = \begin{bmatrix} \mathbf{A}_{F,F}^{(2)} & \mathbf{A}_{F,AR}^{(2)} & \mathbf{A}_{F,WR}^{(2)} \\ \mathbf{A}_{AR,F}^{(2)} & \mathbf{A}_{AR,AR}^{(2)} & \mathbf{A}_{AR,WR}^{(2)} \\ \mathbf{A}_{WR,F}^{(2)} & \mathbf{A}_{WR,AR}^{(2)} & \mathbf{A}_{WR,WR}^{(2)} \end{bmatrix}, \mathbf{q}^{(2)} = \begin{bmatrix} \mathbf{q}^{(1)} \\ \mathbf{q}^{(5)} \\ \mathbf{q}_{WR}^{(2)} \end{bmatrix}, \mathbf{f}^{(2)} = \begin{bmatrix} \mathbf{f}_F^{(2)} \\ \mathbf{f}_{AR}^{(2)} \\ \mathbf{f}_{WR}^{(2)} \end{bmatrix}$$

$$\text{where } \tilde{\mathbf{q}}_{WR}^{(2)} = \begin{bmatrix} \tilde{\theta}^{(3)} \\ \tilde{\theta}^{(4)} \end{bmatrix}$$

- ▶ sub-system 3 (frame – F, cabin – C, driver seat – S)

$$\mathbf{A}^{(3)} = \begin{bmatrix} \mathbf{A}_{F,F}^{(3)} & \mathbf{A}_{F,C}^{(3)} & \mathbf{A}_{F,S}^{(3)} \\ \mathbf{A}_{C,F}^{(3)} & \mathbf{A}_{C,C}^{(3)} & \mathbf{A}_{C,S}^{(3)} \\ \mathbf{A}_{S,F}^{(3)} & \mathbf{A}_{S,C}^{(3)} & \mathbf{A}_{S,S}^{(3)} \end{bmatrix}, \mathbf{q}^{(2)} = \begin{bmatrix} \mathbf{q}^{(1)} \\ \mathbf{q}^{(2)} \\ \mathbf{q}^{(3)} \end{bmatrix}, \mathbf{f}^{(2)} = \begin{bmatrix} \mathbf{f}_F^{(3)} \\ \mathbf{f}_C^{(3)} \\ \mathbf{f}_S^{(3)} \end{bmatrix}$$

For the vehicle model described in such a way an equation of motion was formulated by using of formalism of Lagrange equations of II order. In papers [15, 18] there is a detailed description of mathematical modelling which results in a calculation model and dynamic equations of motion in a matrix form written as:

$$\begin{cases} \mathbf{A}\ddot{\mathbf{q}} - \Phi \mathbf{r} = \mathbf{f} \\ \Phi^T \dot{\mathbf{q}} = \mathbf{w} \end{cases} \quad (12)$$

where:

$$\mathbf{A} = \begin{bmatrix} \mathbf{A}_{F,F}^{(1)} + \mathbf{A}_{F,F}^{(2)} + \mathbf{A}_{F,F}^{(3)} & \mathbf{A}_{F,AF}^{(1)} & \mathbf{A}_{F,SA}^{(1)} & \mathbf{A}_{F,WF}^{(1)} & \mathbf{A}_{F,AR}^{(2)} & \mathbf{A}_{F,WR}^{(2)} & \mathbf{A}_{F,C}^{(3)} & \mathbf{A}_{F,S}^{(3)} \\ \mathbf{A}_{AF,F}^{(1)} & \mathbf{A}_{AF,AF}^{(1)} & \mathbf{A}_{AF,SA}^{(1)} & \mathbf{A}_{AF,WF}^{(1)} & \mathbf{0} & \mathbf{0} & \mathbf{0} & \mathbf{0} \\ \mathbf{A}_{SA,F}^{(1)} & \mathbf{A}_{SA,AF}^{(1)} & \mathbf{A}_{SA,SA}^{(1)} & \mathbf{A}_{SA,WF}^{(1)} & \mathbf{0} & \mathbf{0} & \mathbf{0} & \mathbf{0} \\ \mathbf{A}_{WF,F}^{(1)} & \mathbf{A}_{WF,AF}^{(1)} & \mathbf{A}_{WF,SA}^{(1)} & \mathbf{A}_{WF,WF}^{(1)} & \mathbf{0} & \mathbf{0} & \mathbf{0} & \mathbf{0} \\ \mathbf{A}_{AR,F}^{(2)} & \mathbf{0} & \mathbf{0} & \mathbf{0} & \mathbf{A}_{AR,AR}^{(2)} & \mathbf{A}_{AR,WR}^{(2)} & \mathbf{0} & \mathbf{0} \\ \mathbf{A}_{WR,F}^{(2)} & \mathbf{0} & \mathbf{0} & \mathbf{0} & \mathbf{A}_{WR,AR}^{(2)} & \mathbf{A}_{WR,WR}^{(2)} & \mathbf{0} & \mathbf{0} \\ \mathbf{A}_{C,F}^{(3)} & \mathbf{0} & \mathbf{0} & \mathbf{0} & \mathbf{0} & \mathbf{0} & \mathbf{A}_{C,C}^{(3)} & \mathbf{A}_{C,S}^{(3)} \\ \mathbf{A}_{S,F}^{(3)} & \mathbf{0} & \mathbf{0} & \mathbf{0} & \mathbf{0} & \mathbf{0} & \mathbf{A}_{S,C}^{(3)} & \mathbf{A}_{S,S}^{(3)} \end{bmatrix}$$

– mass matrix,

$\mathbf{q} = [\tilde{\mathbf{q}}^{(1)} \tilde{\mathbf{q}}^{(4)} \tilde{\mathbf{q}}_{SA}^{(1)} \tilde{\mathbf{q}}_{WF}^{(1)} \tilde{\mathbf{q}} \tilde{\mathbf{q}}_{WR}^{(5)} \tilde{\mathbf{q}}^{(2)} \tilde{\mathbf{q}}^{(3)}]^T$ – vector of generalized coordinates of the system,

$$\Phi = \begin{bmatrix} \mathbf{0} & \mathbf{0} & \mathbf{0} & \mathbf{1} & \mathbf{0} & \mathbf{0} & \mathbf{0} & \mathbf{0} & \mathbf{0} \\ \mathbf{0} & \mathbf{0} & \mathbf{1} & \mathbf{0} & \mathbf{0} & \mathbf{0} & \mathbf{0} & \mathbf{0} & \mathbf{0} \end{bmatrix}^T - \text{constraints matrix},$$

$$\mathbf{f} = \left[\mathbf{f}_F^{(1)} + \mathbf{f}_F^{(2)} + \mathbf{f}_F^{(3)} \quad \mathbf{f}_{AF}^{(1)} \quad \mathbf{f}_{SA}^{(1)} \quad \mathbf{f}_{WF}^{(1)} \quad \mathbf{f}_{AR}^{(2)} \quad \mathbf{f}_{WR}^{(2)} \quad \mathbf{f}_C^{(3)} \quad \mathbf{f}_S^{(3)} \right]^T - \text{vector of external, Coriolis and centrifugal forces},$$

$$\mathbf{r} = [\mathbf{r}_1 \quad \mathbf{r}_2]^T - \text{vector of unknown constraint reactions corresponding to torques acting on stub axles connected with the wheels},$$

$$\mathbf{w} = \left[\ddot{\delta}^{(1)} \quad \ddot{\delta}^{(2)} \right]^T - \text{vector of right sides of constraint equations},$$

$\delta^{(i)}$ – steering angle of the i -th front stub axle of the vehicle.

The details of the procedure which lead to form equation (12) with description of elements in matrix \mathbf{A} and vector \mathbf{f} are presented in [18].

3. Optimisation problem

The main aim of optimization is to select such vehicle parameters which provide the best possible driving comfort. In the issue in question the decisive variables determine the parameters of the driver's seat sub-assembly in the discrete time moments:

$$\mathbf{d} = [d_1 \dots d_{n_d}]^T \quad (13)$$

where n_d is a number of the discrete timestamps. Spline functions of the first degree were used to obtain a continuous function of the decisive variables. Additionally, inequality constraints determining the minimum and maximum values of the parameters were considered:

$$d_{\min} \leq d_i \leq d_{\max} \quad (14)$$

These constraints were taken into account in the optimization task by the external penalty function [25, 26], of which value was added to the objective function minimized:

$$\zeta_i(\mathbf{d}) = \begin{cases} 0 & \text{for } g_i(\mathbf{d}) \leq 0 \\ C_{1,i} e^{C_{2,i} g_i(\mathbf{d})} & \text{for } g_i(\mathbf{d}) > 0 \end{cases} \quad (15)$$

where:

$g_i(\mathbf{d}) \leq 0$ dla $i=1, \dots, n_g$ – the inequality constraint defined on basis of (13),

n_g – a number of the inequality constraints,

$C_{1,i}, C_{2,i}$ – weights selected empirically.

In the optimization process there were separate analyses made in which the following functionals were minimized:

- ▶ values of the relative extrema of the driver seat acceleration

$$\Omega_1(\mathbf{d}, \ddot{\mathbf{q}}) = C \sum_{i=1}^{n_e} \left(\ddot{z}^{(3)}(t_{ex,i}) \right)^2 + \sum_{i=1}^{n_s} \zeta_i(\mathbf{d}) \rightarrow \min \quad (16)$$

- ▶ Root Mean Quad (RMQ) of the driver seat acceleration

$$\Omega_2(\mathbf{d}, \ddot{\mathbf{q}}) = \frac{C}{t_e} \sqrt[4]{\int_0^{t_e} \left[\ddot{z}^{(3)}(t) \right]^4 dt} + \sum_{i=1}^{n_s} \zeta_i(\mathbf{d}) \rightarrow \min \quad (17)$$

where:

- n_e – a number of the dominant extrema analyzed in the time course of acceleration of the $\ddot{z}^{(3)}$,
- $t_{ex,i}$ – time moment of i -th extrema of $\ddot{z}^{(3)}$,
- t_e – simulation duration,
- C – weight selected empirically.

Three cases in which the following parameters were subjected to controlling in the driver seat sub-assembly were examined:

- ▶ damping

$$\mathbf{d}_1 = \left[d_1^{(1)} \dots d_i^{(1)} \dots d_{n_d^{(1)}}^{(1)} \right]^T \quad (18)$$

where:

- $d_i^{(1)}$ – a value of driver's seat damping in the discrete time moment t_i ,
- $n_d^{(1)}$ – a number of discrete timestamps,

- ▶ stiffness

$$\mathbf{d}_2 = \left[c_1^{(2)} \dots c_i^{(2)} \dots c_{n_d^{(2)}}^{(2)} \right]^T \quad (19)$$

where:

- $c_i^{(2)}$ – a value of stiffness of the driver seat spring in the discrete time moment t_i ,
- $n_d^{(2)}$ – a number of discrete timestamps,

- ▶ damping and stiffness

$$\mathbf{d}_3 = \begin{bmatrix} \mathbf{d}_1 \\ \mathbf{d}_2 \end{bmatrix} \quad (20)$$

Vector \mathbf{d}_3 contains two vectors (damping and stiffness of the driver seat), and its size is $n_d^{(3)} = n_d^{(1)} + n_d^{(2)}$.

The problem formulated in such a way was solved by Hooke-Jeeves method [25]. The results of the numerical simulations performed for the selected road case and a comparison of the results obtained while conducting the numerical simulations for a few different forms of the objective function and the decisive variables are presented further in the article.

4. Results of numerical calculations

A case in which a vehicle driving at a constant speed drives over an obstacle in a form of speed bumps of 6 cm height (a smooth bump, Fig. 9a) and 10 cm (a sharp bump , Fig. 9b).

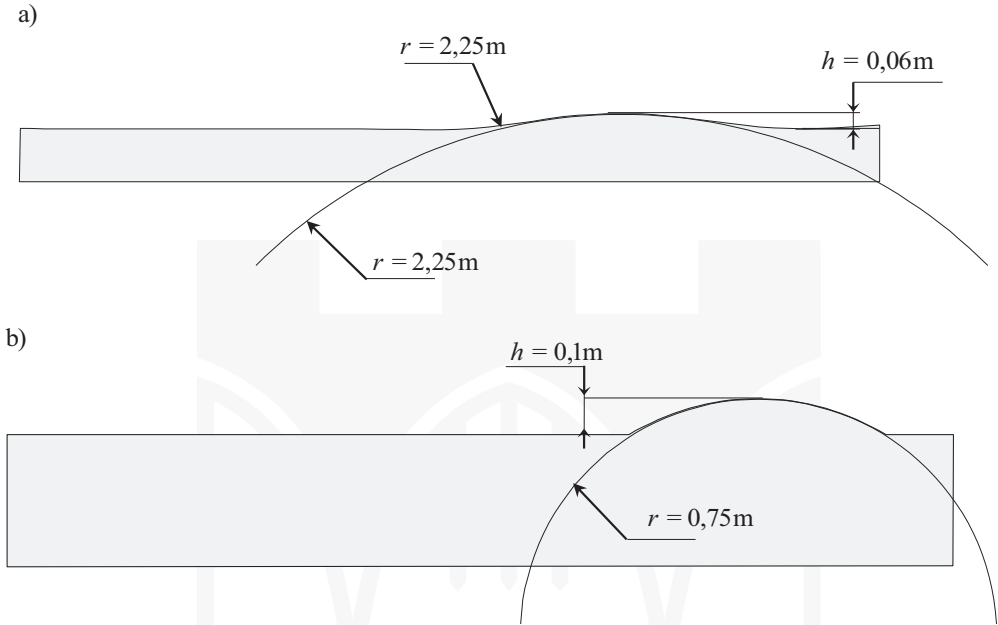


Fig. 9. The profiles of the speed bumps analyzed

An object of the investigations was to determine the optimal coefficients providing a reduction of the driver's seat vibrations while performing the maneuver. In the numerical simulations it has been assumed that the maneuver lasted 3 sec. in which the vehicle drove over the obstacle with the front and rear wheels. The constant speed equal to 10 km/h provided by controlling the driving torque moments and use of a PID regulator [18], was assumed. In the numerical simulations a uniform and non-uniform division of the time interval was tested by increasing a number of points while driving over the obstacle. Finally, it was assumed that the vector of the time moment values can be presented in the form of:

$$\mathbf{t} = (t_i)_{i=1, \dots, n_d} \quad (21)$$

where:

$$t_i = i \frac{t_e}{n_d},$$

$n_d = 15$ – a number of discrete timestamps,

$t_e = 3[s]$ – simulation time.

The physical parameters of the vehicle necessary to perform the simulation were taken from paper [18]. The driver model was accounted in the calculations and dynamic equations of motion as additional mass of 80 kg weight joined with the seat. The constant step Runge-Kutta method of 4-th order [25] was used to integrate equations of motion in each optimization step. The minimal and maximal values of the damping and stiffness coefficients being inequality constraints were taken $d_{z,\min}^{(3)} = 10 \text{ Ns/m}$ and $d_{z,\max}^{(3)} = 4000 \text{ Ns/m}$, $c_{z,\min}^{(3)} = 1 \cdot 10^4 \text{ N/m}$, $c_{z,\max}^{(3)} = 15 \cdot 10^4 \text{ N/m}$, respectively. Fig. 10 presents the results of courses of the decisive variable values for selected solution obtained in the dynamic optimization process where functional (17) and 10 km/h vehicle velocity were assumed.

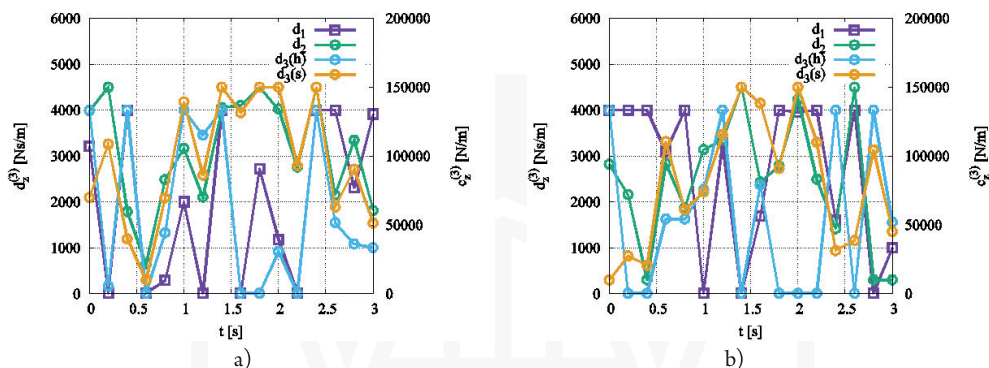


Fig. 10. Courses of the stiffness decisive variables (1), damping (2), stiffness and damping (3) the driver seat obtained in the optimization process for the smooth (a) and sharp (b) bump

Significant differences in the decisive variable courses obtained can be noticed in both cases. The courses obtained for the speed bump of 10 cm height are characterized by higher amplitudes, many a time achieving the upper optimization limit. In spite of differences in the values and the decisive variable courses the subsequent figures show that their usage in the sub-assembly of an active suspension of the seat driver yields desirable effects. Courses of the driver seat acceleration for the different minimized functionals and the decisive variables are presented in Figs 11–13.

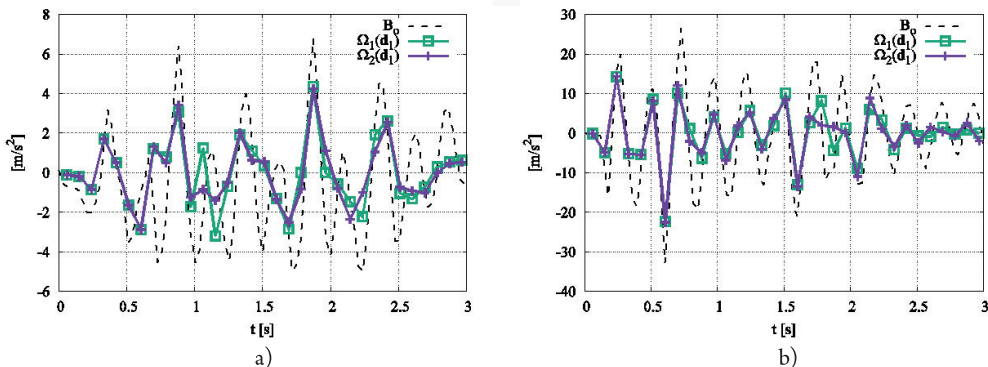
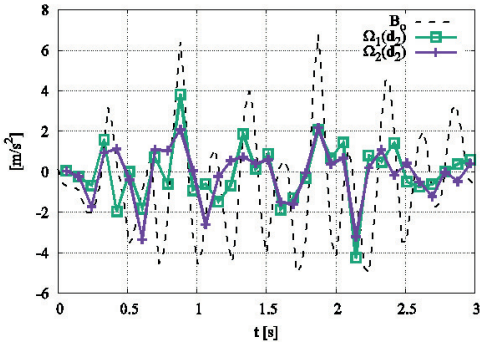
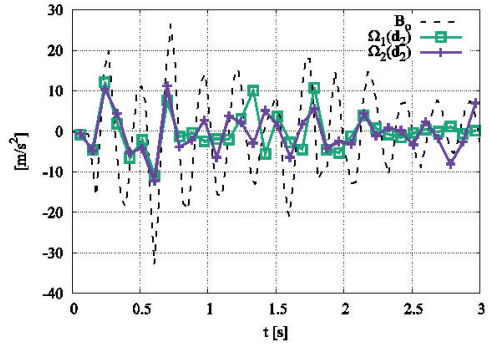


Fig. 11. Courses of the driver's seat acceleration of the damping optimization for the smooth (a) and (b) sharp bump

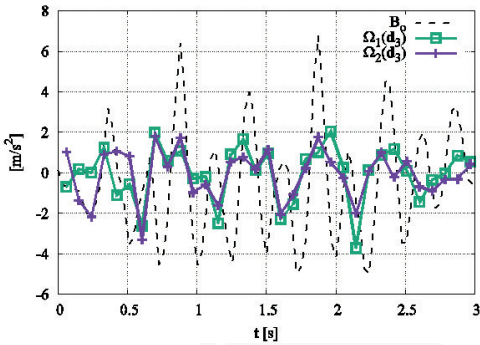


a)

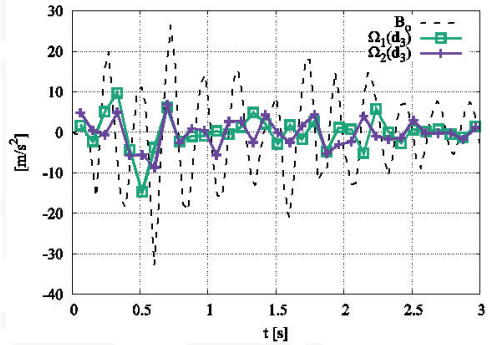


b)

Fig. 12. Courses of the driver's seat acceleration of the spring stiffness optimization for the smooth (a) and sharp (b) bump

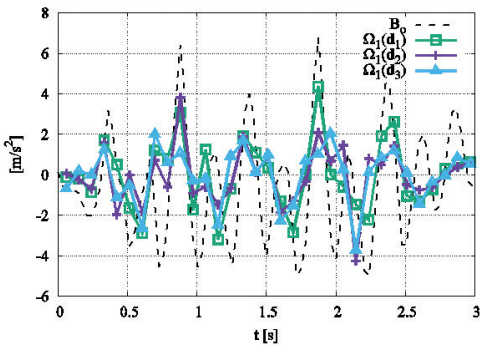


a)

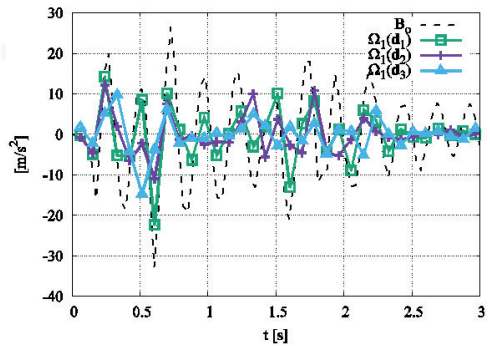


b)

Fig. 13. Courses of the driver's seat acceleration of the damping and spring stiffness optimization for the smooth (a) and sharp (b) bump



a)



b)

Fig. 14. The courses of the driver seat acceleration for the optimized functional Ω_1 and the decisive variables for the smooth (a) and sharp (b) bump

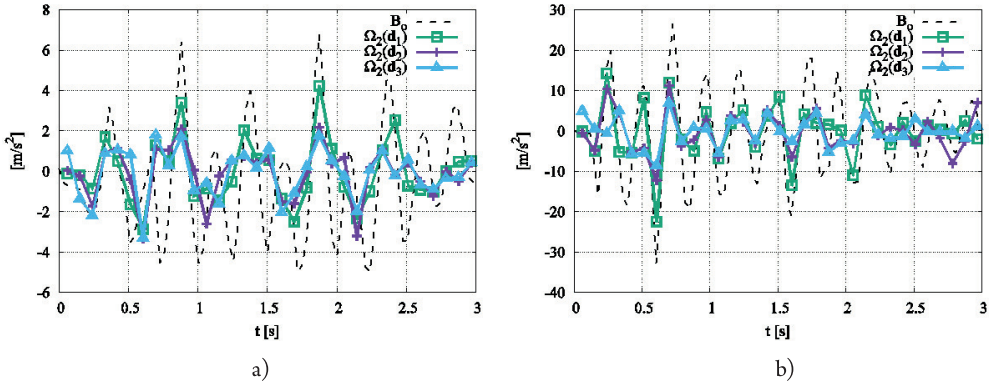


Fig. 15. The courses of the driver seat acceleration for the optimized functional Ω_2 and the decisive variables for the smooth (a) and sharp (b) bump

While analyzing the diagram above it can be noticed that both criteria used to evaluate the objective function value seem to be appropriate in the case analyzed. The Root Mean Quad criterion is slightly better than the criterion examining the relative extrema of the driver seat acceleration. Additionally, the lowest values of the acceleration after the optimization were obtained when both stiffness and driver's seat damping were taken into account in the decisive variable vector. A cumulative list of the courses of the driver seat acceleration for the minimized functional is presented in Figs 14 and 15.

Two indicators were implemented to compare quantitatively the results obtained in the optimization process. The first of them is used to unify a measure of the objective function forms used:

$$\Omega_{ref}(\mathbf{d}_j) = \frac{1}{t_e} \int_0^{t_e} [\ddot{z}^{(3)}(t)]^2 dt + \sum_{i=1}^{n_e} |\ddot{z}^{(3)}(t_{ex,i})| \quad (22)$$

The second indicator which determines a percentage improvement of the driver seat acceleration obtained in the optimization process is described according to the formulae:

$$\Delta_i(\mathbf{d}_j) = \frac{\Omega_{refr} - \Omega_{ef}^{(i,o)}(\mathbf{d}_j)}{\Omega_{ref}^{(i,o)}(\mathbf{d}_j)} \cdot 100\% \quad (23)$$

where:

$\Omega_{ref}^{(s)}$ – the reference value (before the optimization), assuming constant spring stiffness as 90000 N/m and damping 1500 Ns/m,

$\Omega_{ref}^{(i,o)}(\mathbf{d}_j)$ – value of -th objective function after optimization taking -th vector of the decisive variables into account, , .

The values obtained in the optimization process for the different objective functions and the decisive variables are presented in Tables 1 and 2.

Table 1. Values of the objective function and the improvement coefficient obtained from solving the dynamic optimization task for the smooth bump

Objective function	Values of the objective function without optimization $\Omega_{ref}^{(s)}$	Values of the objective function after optimization $\Omega_{ref}^{(i,o)}(\mathbf{d}_j)$	Value of improvement coefficient $\Delta_i(\mathbf{d}_j)$ [%]	Mean value of improvement coefficient [%]
$\Omega_1(\mathbf{d}_1)$	13.94	6.88	50.65	57.25
$\Omega_1(\mathbf{d}_2)$		5.86	57.96	
$\Omega_1(\mathbf{d}_3)$		5.14	63.13	
$\Omega_2(\mathbf{d}_1)$		6.50	53.37	61.45
$\Omega_2(\mathbf{d}_2)$		4.96	64.42	
$\Omega_2(\mathbf{d}_3)$		4.66	66.57	

Table 2. Values of the objective function and the improvement coefficient obtained from solving the dynamic optimization task for the sharp bump

Objective function	Values of the objective function without optimization $\Omega_{ref}^{(s)}(\mathbf{d}_j)$	Values of the objective function after optimization $\Omega_{ref}^{(i,o)}(\mathbf{d}_j)$	Value of improvement coefficient $\Delta_i(\mathbf{d}_j)$ [%]	Mean value of improvement coefficient [%]
$\Omega_1(\mathbf{d}_1)$	153.97	71.10	53.82	67.76
$\Omega_1(\mathbf{d}_2)$		41.19	73.25	
$\Omega_1(\mathbf{d}_3)$		36.22	76.22	
$\Omega_2(\mathbf{d}_1)$		74.18	51.82	69.65
$\Omega_2(\mathbf{d}_2)$		41.35	73.14	
$\Omega_2(\mathbf{d}_3)$		24.63	84.00	

The tabular results confirm an advantage of the Root Mean Quad criterion over the criterion examining the relative extrema of the driver seat acceleration. However, in each case analyzed the improvement coefficient value is greater than 50%. The greatest improvement for the sharp bump, over 80%, can be noticed for the RMQ criterion with use of the vector of the decisive variables containing stiffness and damping of the driver's seat. The mean value of the improvement coefficient confirms the hypothesis that with an increase in the acceleration caused by road unevenness the procedure algorithm presented can improve significantly driving comfort of a special vehicle driver.

5. Conclusions

The article presents a solution to the problem of selecting the parameters of active damping and stiffness of the driver seat by the dynamic optimization, by integrating an equation of motion of the special vehicle in each iteration. The calculations were made for the selected road maneuver with the obstacle in a form of the speed bumps of different height. Two selected objective functions and three variants of the decisive variables were analyzed. The obtained results indicate that a proper selection of both the objective function and the elements subjected to control (stiffness or damping) is very important. The numerical analyses also indicate that with an increase in the acceleration caused by road unevenness, the dynamical optimization conducted properly can improve significantly driving comfort of a driver. An average improvement of about 58% was obtained for driving over the smooth bump and about 68% for driving over the sharp bump. It should be emphasized that the performed studies deal with one road maneuver for two shapes of the speed bumps. However, authors conducted a number of other simulations taking into account the different types of road unevenness and velocity. In this article two unevenness road as an example of effective way of cushioning the driver's seat to determine the stiffness and damping coefficients have been presented. The Hooke-Jeeves method characterized by a great numerical convergence and relatively low sensitivity to a start point was used in the calculations. The presented procedure algorithm is universal and can be applied in other vehicle sub-assemblies and multibody systems. In this article presented algorithm improves significantly driving comfort of a special vehicle driver, although due to long time of calculations it can be used only to verify the existing controllers operating in the real time. In subsequent works the authors plan to use an artificial neuron network. After appropriate training the neuron network can be implemented in the controller of the active driver seat damping system to select the optimum parameters in the real time. For this purpose a number of maneuvers and shapes of road unevenness should be increased to collect data for an artificial neuron networks training set.

References

- [1] Guglielmino E., Sireteanu T., Stammers C.W., Ghita G., Giu-clea M., *Semi-active Suspension Control, Improved Vehicle Ride and Road Friendliness*, Springer-Verlag, London 2008.
- [2] Sammonds G., Fray M., Mansfield N., *Overall car seat discomfort onset during long duration driving trials*, Advances in Physical Ergonomics and Human Factors Part II, AHFE Conference Books, 2014, 25–35.
- [3] Yang S., Chen L., Li S., *Dynamics of Vehicle-Road Coupled System*, Springer-Verlag, Berlin 2015.
- [4] Jamrozik K., Kosobudzki M., Ptak J., *Assessment of the comfort of passenger transport in special purpose vehicles*, Eksploatacja i Niezawodność – Maintenance and Reliability, 15 (1), 2013, 25–30.

- [5] Chimote K., Gupta M., *Integrated Approach Of Ergonomics And Fem Into Truck Drivers Seat Comfort*, 1st International and 16th National Conference on Machines and Mechanisms, IIT Roorkee, 2013, 183–188.
- [6] Mircheski I., Kandikjan T., Sidorenko S., *Comfort analysis of vehicle driver's seat through simulation of the sitting process*, Tehnički vjesnik 21, 2014, 291–298.
- [7] Gunther P., Pendlebury J., Miller J., *The contribution of seat components to seat hardness and the interface between human occupant and a driver seat*, International Journal of Human Factors Modelling and Simulation, 2012, 378–397.
- [8] Holen P., Thorvald B., *Possibilities and limitations with distributed damping in heavy vehicles*, Vehicle System Dynamics Supplement 41, 2004, 172–181.
- [9] Rao K., Kumar S., *Modeling and Simulation of Quarter Car Semi Active Suspension System Using LQR Controller*, Proceedings of the 3rd International Conference on Frontiers of Intelligent Computing: Theory and Applications (FICTA), Springer-Verlag, 2015, Vol. 1, 441–448.
- [10] Savaresi S., Poussot-Vassal C., Spelta C., Senname O., Dugard L., *Semi-Active Suspension Control Design for Vehicles*, Elsevier Ltd., 2010.
- [11] Lozia Z., Zdanowicz P., *Optimization of damping in the passive automotive suspension system with using two quarter-car models*, Scientific Conference on Automotive Vehicles and Combustion Engines (KONMOT 2016), Vol. 148, No. 1, 2016.
- [12] Zhu X., Zhu S., *A Theoretical Model for Calculating Vibration Characteristics of A Kind of Driver Seat with Air Spring and MR Damper*, Applied Mechanics and Materials, Vol. 141, 2012, 8–14.
- [13] Rezaee M., Osguei A., Arghand H., *An investigation on the ride comfort of a vehicle subjected to the random road excitation*, International Journal of Vehicle Safety 6(3), 2013, 235–253.
- [14] Attia E. M., Ayman F. Z., El Gamal H.A., El Souhily B.M., *Effect of Irregular Road on Dynamic Response of Car Seat Suspended by a Magneto-Rheological (MR) Damper*, International Journal of Applied Science and Technology, 2014, No. 5, Vol. 4, 39–54.
- [15] Warwas K., *Analiza i sterowanie ruchem pojazdów wieloczołonowych z uwzględnieniem podatności elementów*, PhD Thesis, Faculty of Mechanical Engineering and Computer Science, University of Bielsko-Biala, 2009.
- [16] Warwas K., Augustynek K., *Dynamic optimisation of articulated vehicle motion for control of stability in critical situation*, IDAACS 2015: 8th IEEE International Conference on Intelligent Data Acquisition and Advanced Computing Systems: Technology and Applications, Vol. 1, 2015, 232–237.
- [17] Tengler S., Warwas K., *Aktywne tłumienie siedzenia pojazdu specjalnego, 55 Sympozjon, Modelowanie w mechanice, Ustroń 2016*.
- [18] Tengler S., *Analiza dynamiki samochodów specjalnych o wysoko położonym środku ciężkości*, PhD Thesis, Faculty of Mechanical Engineering and Computer Science, University of Bielsko-Biala, 2012.
- [19] Tengler S., *Dynamic analysis of special cars on uneven roads*, ECCOMAS Congress 2016 VII European Congress on Computational Methods in Applied Sciences and Engineering, Eds. M. Papadrakakis, V. Papadopoulos, G. Stefanou, V. Plevris, Crete Island, Greece, 5–10 June 2016.

- [20] Fiala E., *Lateral forces at the rolling pneumatic tire*, Technische Hochschule, 1954.
- [21] Mitraa A., Desaib G., Patwardhanc S., Shirked P., Kurnee W., Banerjee N., *Optimization Of Passive Vehicle Suspension System By Genetic Algorithm*, Procedia Engineering 144, 2016, 1158–1166.
- [22] Abbas W., Abouelatta O., El-Azab M., M. El-Saidy, Megahed A., *Genetic algorithms for the optimal vehicle's driver-seat suspension design*, Journal of Mechanics Engineering and Automation 1, 2011, 44–52.
- [23] Badran S., Salah A., Abbas W., Abouelatta O., *Design of Optimal Linear Suspension for Quarter Car with Human Model using Genetic Algorithms*, The Research Bulletin of JORDAN ACM, Vol. II (II), 2011, 142–151.
- [24] Grzegożek W., Adamiec-Wójcik I., Wojciech S., *Komputerowe Modelowanie Dynamiki Pojazdów Samochodowych*, Wydawnictwo Politechniki Krakowskiej, 2003.
- [25] Press W., Teukolsky W., Vetterling S., Flannery W. B., *Numerical Recipes 3rd Edition: The Art of Scientific Computing*, Cambridge University Press, Cambridge 2007.
- [26] Paulavičius R., Žilinskas J., *Simplicial Global Optimization*, Springer-Verlag, New York 2014.

